A Novel Direct Duty-to-Current Control for DC Bias Mitigation in Dual Active Bridge Converters for Enhanced EV Applications

Moneeba Gulzar Utah State University Logan, USA Ramish Majeed Raja *Utah State University* Logan, USA Regan Zane
Utah State University
Logan, USA

Hongjie Wang Utah State University Logan, USA

Abstract—This paper presents a novel direct duty-to-current control strategy to mitigate the dc bias and eliminate the need for a dc blocking capacitor in Dual Active Bridge (DAB) converters. The proposed control mechanism directly controls the duty cycle of each leg in the primary H-bridge to regulate the average (over one switching period) volt-seconds applied to the transformer primary winding to be zero without a dc blocking capacitor, under both steady-state and transient operations. This strategy is particularly relevant for electric vehicle (EV) applications, where variations in power demand and charging protocols can introduce dc bias, and the proposed control strategy work seamlessly with the output voltage control loop, during both steady-state operation and transients. The analysis, presented in detail, includes simulation results validating the effectiveness of the proposed control strategy under various steady-state and transient conditions, demonstrating its robustness and applicability in EV systems.

Index Terms—Dual active bridge (DAB) converter, duty-tocurrent control, transformer saturation, electric vehicles (EVs)

I. INTRODUCTION

The growing demand for EVs has led to significant advancements in its infrastructure, with dual active bridge (DAB) converters emerging as a popular choice for EV applications. The DAB converter is favored due to its high efficiency, bidirectional power flow capability, galvanic isolation, and wide soft-switching range [1]–[6]. Additionally, the DAB's ability to operate effectively over a wide range of input and output voltages, high power density, and easy control implementation makes it suitable for varying battery states and charging protocols, which are essential features for modern EV applications [7]–[9].

However, one of the challenges associated with DAB converters is the potential introduction of dc bias in the transformer windings. The dc bias current in a DAB converter can occur both in steady state and transient conditions, particularly during dynamic operations such as start-up, load changes, or power flow direction shifts [10]. The root causes of dc bias current include inconsistencies in semiconductor manufacturing, variations in the time delays of gating driver signals, mismatched switching times, and abrupt changes in terminal voltage [11], [12]. Excessive dc bias can lead to a nonzero average inductor current, which, when passing through the transformer, causes the magnetization curve to lose its

symmetry and potentially results in core saturation in one direction. If left unchecked, this can increase core losses, impact power transfer, and damage electrical equipment [13], [14]. Therefore, eliminating dc bias is crucial for maintaining the efficiency and longevity of DAB converters in EV applications.

Several methods have been proposed in the literature to address dc bias in DAB converters. One common approach is the use of a dc blocking capacitor in series with the transformer. While this method is straightforward, a large number of parallel connected capacitors are required, which introduces additional components, increases the system's volume and cost, and the resulting low-frequency oscillations may negatively impact the power density and dynamic response of the converter [15].

Another technique involves rapid control and peak current management [16]. This method is notable for eliminating the dc bias by accelerating the transient time but adds auxiliary circuits to the EVs.

More advanced methods include the implementation of optimal control schemes employing triple-phase-shift (TPS) and extended phase shift (EPS) to regulate the change in inductor current [17], [18]. These methods offer more control freedom; however, the calculations become complex, and hard switching during transients is inevitable. This issue is more prominent in high-frequency applications of wide bandgap devices, making implementation in the dynamic environment of EVs challenging [14]. The proposed direct duty-to-current control strategy in this paper offers a novel solution by directly controlling the duty cycle of each leg in the primary H-bridge. This approach regulates the average volt-seconds applied to the transformer primary winding to be zero, eliminating the need for a dc blocking capacitor or auxiliary circuits. The proposed method streamlines the converter's architecture and reduces physical size and cost by reducing the need for large dc-blocking capacitors. This makes the design more economical and energy-efficient for EV applications. Unlike traditional methods, this strategy maintains performance under both steady-state and transient conditions without impacting the performance of the output voltage control loop. The system retains independence between the current and voltage controllers. This separation allows each controller to operate within its bandwidth, enabling the current controller to func-

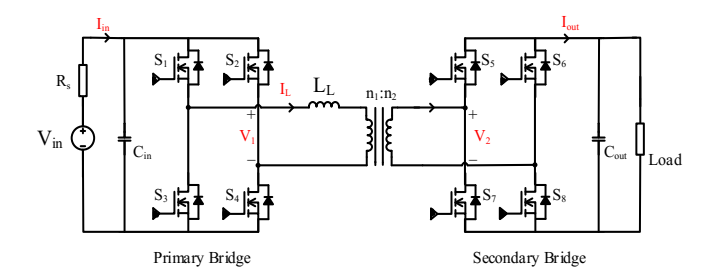


Fig. 1. Circuit diagram of a traditional dual active bridge (DAB) converter.

tion efficiently under diverse conditions, such as substantial dc biases and changes in output reference voltage and loads, making it suitable for EVs.

This paper presents detailed modeling and analysis of the proposed control strategy, with simulation results demonstrating its effectiveness in mitigating dc bias and ensuring stable operation, including scenarios with significant changes in load and voltage. The simplicity, effectiveness, and adaptability of the proposed method make it a promising solution for future EV application. In this paper, Section II discusses the steady-state operation of DAB converter topology. Section III provides a detailed analysis and methodology of the proposed current-to-duty control. Section IV includes simulation results and validates our direct current-to-duty control approach under various steady-state and transient conditions, and Section V concludes the paper.

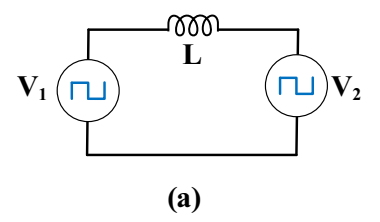
II. DUAL ACTIVE BRIDGE CONVERTER

A traditional DAB converter, as depicted in Figure. 1, is utilized in this study. The DAB converter consists of two H-bridges, one on the primary side and one on the secondary side, connected through a high-frequency transformer. This configuration allows for bidirectional power transfer with galvanic isolation and is highly suitable for EV application. Figure. 2(a) illustrates the simplified circuit of the DAB converter where two square voltage sources (V_1 and V_2) are considered, with an inductive element in between. The primary side H-bridge generates the square wave voltage V_1 , while the secondary side H-bridge generates V_2 . The phase shift between these voltages controls the power flow through the inductive element, allowing precise control of power.

A. Steady State Analysis

Figure. 2(b) shows the steady-state voltages of the primary and secondary bridges and the resulting inductor current, i_L . Analyzing these waveforms helps in understanding the converter's operation under steady-state conditions. The inductor current can be divided into intervals based on the switching periods of the primary and secondary voltages. During these intervals, the inductor current equation is determined by integrating the voltage difference across the inductor.

The inductor current equation, considering the waveforms in Figure. 2(b), is derived as



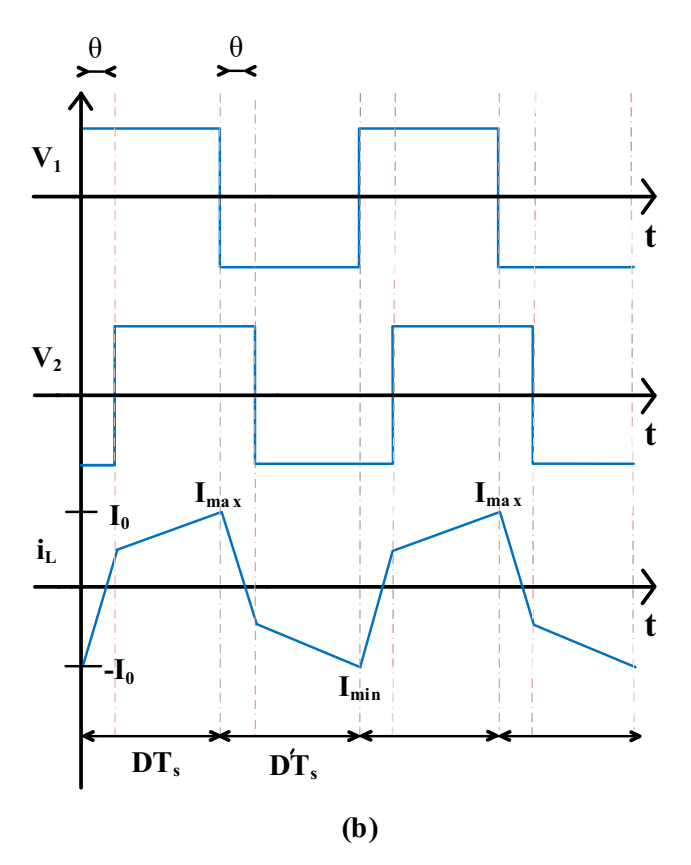


Fig. 2. DAB converter. (a) Simplified circuit. (b) Waveforms.

$$i_{L}(t) = \begin{cases} \frac{V_{1}+V_{2}}{L}t - I_{0} \\ \frac{V_{1}-V_{2}}{L}t + \frac{V_{1}+V_{2}}{L}\theta - I_{0} \\ -\frac{V_{1}+V_{2}}{L}t + \frac{V_{1}-V_{2}}{L}(DT_{s}-\theta) + \frac{V_{1}+V_{2}}{L}\theta - I_{0} \\ -\frac{V_{1}-V_{2}}{L}t + \frac{V_{1}-V_{2}}{L}(DT_{s}-\theta) - I_{0} \end{cases}, \quad (1)$$

where $I_{\rm o}$ is the initial inductor current, L is the inductance of the topology, $V_{\rm 1}$ is the primary H-bridge voltage, $V_{\rm 2}$ is the secondary H-bridge voltage, θ is the phase shift between the primary and secondary H-bridges, DT_s is the first portion, and $D'T_s$ is the other portion of the switching period, as shown in Figure. 2(b).

The minimum and maximum inductor current peaks are evaluated at 0 and DT_s respectively, as

$$I_{\min} = i_L(0) = -I_{\rm o},$$
 (2)

$$I_{\text{max}} = i_L(DT_s) = \frac{V_1 - V_2}{L}(DT_s) + \frac{V_1 + V_2}{L}\theta - I_0,$$
 (3)

The above mentioned equations capture the impact of converter parameters such as bridge voltages, phase shift, and switching periods, and form the basis for developing control strategies to mitigate dc bias current, as discussed in the subsequent section.

III. PROPOSED CONTROLLER

In DAB converters, traditionally, the presence of dc bias is typically analyzed by examining the symmetry of the inductor current over a switching cycle. A zero dc bias current is indicated by equal positive and negative areas of the inductor current. One effective method to verify this symmetry, and thus confirm zero dc bias current, is to ensure that the positive and negative peaks of the inductor current are equal.

Therefore, a DAB converter exhibiting dc bias means $|I_{\min}| \neq I_{\max}$. In this work, the sum of the peaks, denoted as I_{sum} (derived using Equations (1) – (3)), is calculated at every switching cycle using

$$I_{\text{sum}} = I_{\text{max}} + I_{\text{min}},\tag{4}$$

$$I_{\text{sum}} = \frac{V_1 - V_2}{L} (DT_s) + \frac{V_1 + V_2}{L} \theta - 2I_0, \tag{5}$$

It can be seen from (5) that the duty cycle directly affects the magnetic bias current of the DAB. Hence, duty cycles of the half-bridge legs in the primary side bridge can be directly used to control the current I_{sum} . The above linearized equation has a steady-state operating point as $I_{\text{sum},0}$, D_0 , and θ_0 . The small signal transfer function from the duty cycle to the inductor current peaks sum (I_{sum}) can be derived by replacing I_{sum} , D, and θ using

$$I_{\text{sum}} = I_{\text{sum},0} + \Delta \hat{I}_{\text{sum}},\tag{6}$$

$$D = D_0 + \Delta \hat{d},\tag{7}$$

$$\theta = \theta_0 + \Delta \hat{\theta}. \tag{8}$$

Substituting $\Delta \hat{I}_{\text{sum}}$ and $\Delta \hat{d}$ perturbations into (5) and taking the Laplace transform, $G_{I_{\text{sum}}d}$ can be derived as

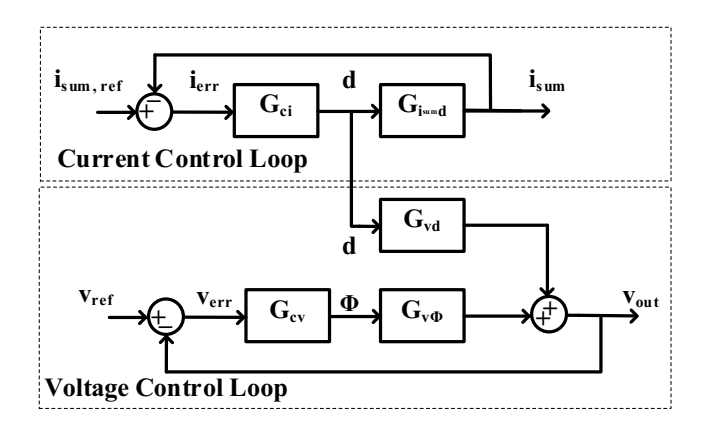


Fig. 3. Control diagram of proposed dc bias current correction strategy for DAB along with output voltage control.

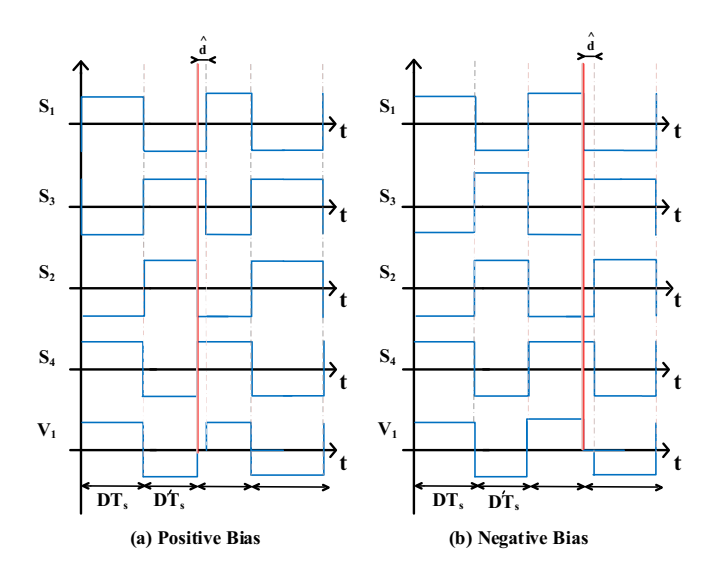


Fig. 4. Illustrates the proposed control strategy for mitigating (a) positive dc bias by reducing the duty cycle of switch S_1 , and (b) negative dc bias by reducing the duty cycle of switch S_3 in the primary H-bridge of the DAB converter. The red line indicates the starting point of dc bias in the system.

$$G_{I_{\text{sum}}d} = \frac{\Delta \hat{I}_{\text{sum}}}{\hat{d}} = \frac{(V_1 - V_2)}{L f_s}.$$
 (9)

With the above-derived small-signal transfer function, a PI controller can be designed to regulate the dc bias current, as shown in the system control diagram in Figure. 3. In Figure. 3, the $I_{\text{sum,ref}}$ is typically zero to eliminate the dc bias current.

A. Methodology

The current-to-duty controller response is applied to the four switches of the primary H-bridge, named S_1 , S_2 , S_3 , and S_4 , as shown in Figure. 1. The switching scheme in this paper ensures that S_1 and S_3 are complementary, as are S_2 and S_4 . This arrangement prevents both upper or lower switches from being on simultaneously, which would draw a large current from the source and result in significant power loss.

Conventionally, in the single-phase shift modulation of DAB, these switches are set to a 50% duty cycle, as shown in Figure 4(a) and 4(b) (before the red line). The red line represents the instance when either a positive or negative dc bias is introduced in the system. In Figure 3, the output (duty cycle d) from the PI controller (G_{ci}) represents the required change in the duty cycle of the primary H-bridge output voltage. This change shifts the duty cycle from 50% to a range between 48% and 52%, determined after rigorous simulations to ensure minimal impact on power transfer. Based on the controller output, the control strategy adjusts the duty cycle of the corresponding half-bridge leg in the primary H-bridge, as shown in Figure 4(a) and 4(b) after the red line. For example, in the case of a positive bias, the controller reduces the duty cycle of switch S_1 and maintains S_2 at 50% duty cycle. These adjustments make V_1 positive for less than 50% of the duty cycle while keeping the negative duration at 50%, resulting

in more negative current per cycle compared to positive, thus counterbalancing the positive bias current.

In summary, the controller creates asymmetry in the inductor voltage that induces a counterbalancing current to neutralize the bias. As shown in Figure. 3, a weak coupling (G_{vd}) between the dc bias current control loop and the output voltage control loop exists in the system. However, the interactions between the two loops are minimized by limiting the delta duty cycle to only 2% and having different bandwidths for the two control loops. The simulation results validate this approach, demonstrating effective dc bias mitigation and system stability under various conditions.

IV. SIMULATION RESULTS

To validate the effectiveness of the proposed controller for mitigating dc bias in DAB converters, comprehensive simulations were conducted. The primary objectives of these simulations were to evaluate the controller's performance in eliminating dc bias current and to assess its impact on overall system stability and output voltage regulation.

A. Simulation Setup

The simulation model was developed using PLECS, with parameters and operating conditions given in Table I. Intentionally a significant positive and negative dc bias of 0.1 V was introduced, which is much higher than the typical millivolt biases used in standard tests. Additionally, the independence of the controllers G_{ci} and G_{cv} is evaluated by observing the inductor current (I_L) , output voltage (V_{out}) , output power (P_{out}) , and average inductor current (I_{Lavg}) , under four different cases. The dc bias is added in the first two cases, and V_{out} and P_{out} are varied across the subsequent cases to assess the performance and interaction of the controllers under dynamic conditions.

_	
Parameter	Value
Input Voltage (V_g)	200 V
Output Voltage (V_{out})	150 V
Switching Frequency (f_s)	50 kHz
Inductance (L)	83 µH
Transformer Turns Ratio	1:1
Output Power (P_{out})	480 W

TABLE I Initial Simulation Parameters

B. Case 1: Positive dc Bias Introduction

In the first case, $0.06s \leq t < 0.12s$, a positive bias of $0.1~\rm V$ is introduced as shown in Figure. 5(c). This simulates a scenario where external factors, such as component imperfections or change of load from light to heavy load, introduce a positive bias in the DAB [1]. Upon introducing the $0.1~\rm V$ dc bias at t=0.06s, a disruption in the volt-second balance is observed, leading to an increase in the inductor current from $5.8~\rm A$ to $6~\rm A$, hence creating a non-zero $I_{L_{\rm avg}}$. The controller adjusts DAB by reducing the on and off time of switches S_1 and S_3 respectively, restoring the volt-second balance and ensuring $I_{L_{\rm avg}}$ remains at zero.

C. Case 2: Negative dc Bias Introduction

In the second case, $0.12s \le t \le 0.33s$, a negative bias of 0.1 V is added at 0.12 seconds and remains in the system for the remainder of the simulation, as shown in Figure. 5(c). This case represents potential negative bias scenarios in EV systems, such as regenerative braking or decrease of load [1]. The controller successfully eliminates the negative bias and maintains system stability. The controller's adjustment in response to the negative bias ensures the $I_{L_{\rm avg}}$ remains at zero, preventing transformer core saturation.

In the simulations, the initial condition shows the inductor current symmetrically distributed around zero with no dc bias. Throughout this process, the V_{out} and P_{out} remain steady at 150V and 480W respectively, illustrating the successful independent operation of the controllers G_{ci} and G_{cv} . They manage to perform their respective functions—dc bias elimination and voltage regulation—without interfering with each other. This is because the duty adjustments are so small that they do not affect the $G_{v_{out}d}$ response, which connects the voltage control and current control. This demonstrates the controllers' ability to handle disturbances while maintaining system stability and performance.

D. Case 3: Voltage Reference Change from 150 V to 140 V

In this scenario, $0.18s \le t \le 0.33s$, the reference voltage for the DAB output is reduced from 150 V to 140 V. This situation is similar to adjustments in the output voltage required for different charging protocols or battery management systems in EVs. During such voltage reference changes, the currentto-duty control method removes any dc bias that may be introduced, ensuring the DAB converter continues to operate efficiently and reliably without affecting the desired voltage change. The G_{cv} controller regulates the output voltage to the new reference value of 140 V, resulting in a decrease in output power from 480 W to 418 W, against a persistent -0.1 V external dc bias from Case 2. This voltage change leads to a transient minor dip in I_L and a slight increase in $I_{L_{\mathrm{avg}}}$ by 0.02 A, yet I_L stabilizes at steady state values of I_{max} and I_{min} as per equations 2 and 3, with $I_{L_{avg}}$ remaining close to zero. This ensures the absence of dc bias in the inductor current and demonstrates the $G_{I_{\text{sum}}d}$ effectiveness in eliminating dc bias without disrupting the voltage regulation process.

E. Case 4: Power Level Change from 480 W to 520 W

In this scenario, $0.24s \le t \le 0.33s$, the system's power level is increased from 480 W to 520 W, against a persistent -0.1 V external dc bias from Case 2, and with a new V_{out} of 140 V from Case 3, by decreasing the load resistance from 47 Ω to 38 Ω as shown in Figure. 5(e). This is analogous to variations in power demand in EV applications. For instance, if an EV experiences a sudden increase in power demand due to acceleration or additional loads, the DAB converter must adapt to the new power level. This change in power level induces transients in V_{out} , I_L , and $I_{L_{avg}}$, with V_{out} initially

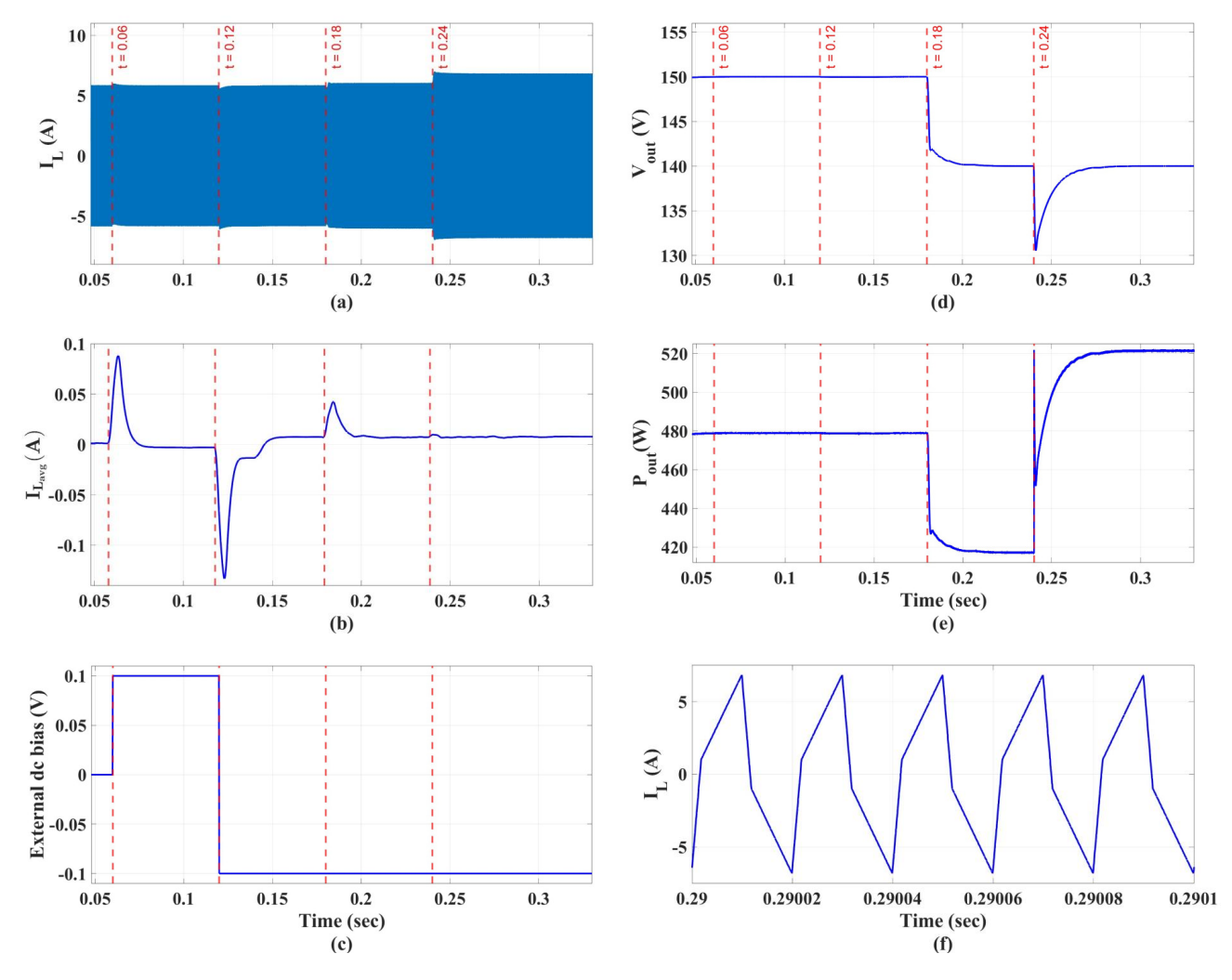


Fig. 5. Shows the system response under 0.1V external dc bias $(0.06s \le t < 0.12s)$, -0.1V external dc bias $(0.12s \le t \le 0.33s)$, output reference voltage change from 150V to 140V $(0.18s \le t \le 0.33s)$, output power change from 418W to 520W $(0.24s \le t \le 0.33s)$ and steady-state inductor current. Figure (a) to (f) are as follows: (a) inductor current I_L , (b) average inductor current $(I_{L_{avg}})$, (c) external dc bias, (d) output voltage (V_{out}) , (e) output power (P_{out}) and (f) steady-state inductor current.

dropping then regulating back at 140 V through the voltage control, and I_L increasing from 6 A to 7 A to meet the new load demands. $I_{L_{\rm avg}}$ temporarily increases to 0.005 A before reaching its reference value, all efficiently managed by the G_{ci} controller. This underscores the controller's efficiency in adapting to power level changes, ensuring the DAB system's stability and countering dc bias.

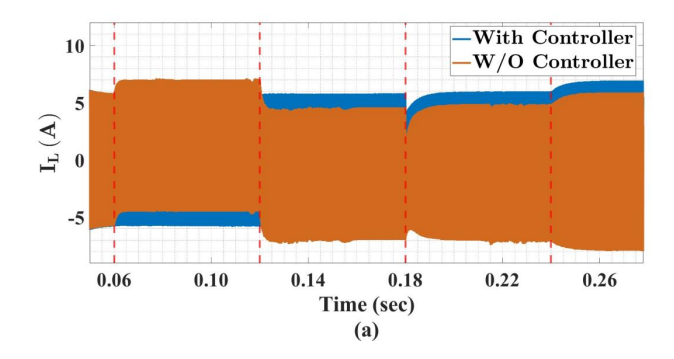
The effects of these cases on I_L and V_{out} are shown in Figs. 5(a) and 5(d). Additionally, it is important to note that a zero bias implies a zero average of inductor current at every switching cycle. Figure. 5(b) shows a moving average of the inductor current, calculated over 40 switching cycles. This visualization aids in understanding the impact of the addition of dc bias, the change in output reference voltage V_{ref} , and the power level of the DAB on I_L . Figure. 5(f) shows a steady state inductor current at 0.29 s, demonstrating a zero dc current in the inductor even after the four cases.

F. DAB response with and without proposed controller

This work also compares the DAB response with and without the proposed controller under the four cases. The results are shown in Figure 6. Figure 6(a) presents the inductor current waveform, while Figure 6(b) illustrates the average inductor current. In both figures, the blue line represents the response with the controller, G_{ci} , and the brown line represents the response without the controller.

Without the controller, introducing a positive bias causes the inductor current waveform to continuously increase in the positive direction. Conversely, introducing a negative bias shifts the overall waveform to a negative level. During dynamic operations (cases 3 and 4), transients add DC bias to the system. This overall DC bias causes asymmetry in the transformer magnetization curve, potentially leading to transformer core saturation.

In contrast, our proposed controller G_{ci} effectively mitigates



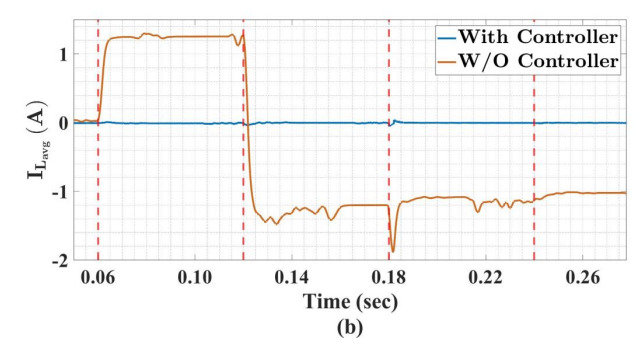


Fig. 6. Comparison of DAB response with and without the proposed controller G_{ci} under 0.1V external dc bias $(0.06s \le t < 0.12s)$, -0.1V external dc bias $(0.12s \le t \le 0.33s)$, output reference voltage change from 150V to 140V $(0.18s \le t \le 0.33s)$, output power change from 418W to 520W $(0.24s \le t \le 0.33s)$. (a) inductor current I_L , (b) average inductor current I_{Lavg}

this dc bias across all four cases, as shown by the zero $I_{L_{\rm avg}}$ in Figure. 6(b). The controller maintains the symmetry of the transformer core and ensures stable operation. This makes our controller valuable for enhancing the reliability and performance of EV infrastructure.

V. CONCLUSION

In summary, the proposed novel direct duty-to-current control strategy demonstrated robust performance under various steady-state and transient conditions involving significant dc biases and changes in V_{out} and P_{out} . The PLECS simulation results confirmed the controller's ability to effectively mitigate dc biases and maintain system stability without affecting the core functionalities of the DAB, such as voltage regulation and power level adjustment. This is particularly significant for EV applications, where the control strategy can handle variations in power demand and charging protocols, ensuring efficient and reliable operations without the need for a dc blocking capacitor.

REFERENCES

- Qinglei Bu, Huiqing Wen, Haochen Shi, and Yinxiao Zhu. A comparative review of high-frequency transient dc bias current mitigation strategies in dual-active-bridge dc-dc converters under phase-shift modulations. *IEEE Transactions on Industry Applications*, 58(2):2166–2182, 2022
- [2] Haifeng Fan and Hui Li. High-frequency transformer isolated bidirectional dc-dc converter modules with high efficiency over wide load range for 20 kva solid-state transformer. *IEEE Transactions on Power Electronics*, 26(12):3599–3608, 2011.
- [3] Haochen Shi, Huiqing Wen, Jie Chen, Yihua Hu, Lin Jiang, Guipeng Chen, and Jieming Ma. Minimum-backflow-power scheme of dabbased solid-state transformer with extended-phase-shift control. *IEEE Transactions on Industry Applications*, 54(4):3483–3496, 2018.
- [4] Biao Zhao, Qiang Song, Wenhua Liu, and Yandong Sun. Overview of dual-active-bridge isolated bidirectional dc-dc converter for highfrequency-link power-conversion system. *IEEE Transactions on Power Electronics*, 29(8):4091–4106, 2014.
- [5] Hua Bai and Chris Mi. Eliminate reactive power and increase system efficiency of isolated bidirectional dual-active-bridge dc-dc converters using novel dual-phase-shift control. *Power Electronics, IEEE Transac*tions on, 27:2905 – 2914, 12 2008.
- [6] Florian Krismer and Johann W. Kolar. Efficiency-optimized highcurrent dual active bridge converter for automotive applications. *IEEE Transactions on Industrial Electronics*, 59(7):2745–2760, 2012.

- [7] J. V. G. Rama Rao and S. Venkateshwarlu. Soft-switching dual active bridge converter-based bidirectional on-board charger for electric vehicles under vehicle-to-grid and grid-to-vehicle control optimization. *Journal of Engineering and Applied Science*, 71(1), February 2024.
- [8] Subhasis Nayak, Anandarup Das, Raymundo E. Torres-Olguin, Salvatore D'Arco, and Giuseppe Guidi. Battery energy support to cascaded hbridge converter fed large scale pv system during unbalanced power generation. In 2020 International Conference on Power, Instrumentation, Control and Computing (PICC), pages 1–6, 2020.
- [9] Gierri Waltrich, Marcel A. M. Hendrix, and Jorge L. Duarte. Threephase bidirectional dc/dc converter with six inverter legs in parallel for ev applications. *IEEE Transactions on Industrial Electronics*, 63(3):1372– 1384, 2016.
- [10] Haochen Shi Qinglei Bu, Huiqing Wen and Yinxiao Zhu. A comparative review of high-frequency transient dc bias current mitigation strategies in dual-active-bridge dc-dc converters under phase-shift modulations. IEEE Transactions on Industry Applications, 58(2):2166–2180, 2022.
- [11] IEEE Lukas Fassler Johann Walter Kolar Gabriel Ortiz, Member and Oscar Apeldoorn. Flux balancing of isolation transformers and application of "the magnetic ear" for closed-loop volt-second compensation. IEEE Transactions on Power Electronics, 29(8):4078–4090, 2014.
- [12] Biao Zhao, Qiang Song, Wenhua Liu, and Yuming Zhao. Transient dc bias and current impact effects of high-frequency-isolated bidirectional dc-dc converter in practice. *IEEE Transactions on Power Electronics*, 31(4):3203–3216, 2016.
- [13] Guanqun Qiu, Li Ran, Hao Feng, Huaping Jiang, Teng Long, Andrew J. Forsyth, WeiHua Shao, and Xu Hou. A fluxgate-based current sensor for dc bias elimination in a dual active bridge converter. *IEEE Transactions on Power Electronics*, 37(3):3233–3246, 2022.
- [14] Xu Han, Huiqing Wen, Qinglei Bu, Yinxiao Zhu, Zhichen Feng, Guangyu Wang, Shahamat Shahzad Khan, Wen Liu, Jiafeng Zhou, and Yong Yang. Transient dc-bias and hard-switching mitigation for fast power reversal in dual-active-bridge dc-dc converters. *IEEE Transactions on Industry Applications*, 60(3):4025–4037, 2024.
- [15] R. Redl, N.O. Sokal, and C.W. Schaefer. Transformer saturation and unusual system oscillation in capacitively coupled half-bridge or fullbridge forward converters: causes, analyses, and cures. In PESC '88 Record., 19th Annual IEEE Power Electronics Specialists Conference, pages 820–829 vol.2, 1988.
- [16] Nimrod Vazquez and Marco Liserre. Peak current control and feedforward compensation of a dab converter. *IEEE Transactions on Industrial Electronics*, 67(10):8381–8391, 2020.
- [17] Tianli Dai, Jinggang Qin, Gao Ge, Chao Zhou, Lican He, Jingyu Zhai, and Jiangang Li. Research on transient dc bias analysis and suppression in eps dab dc-dc converter. *IEEE Access*, 8:61421–61432, 2020.
- [18] Qinglei Bu, Huiqing Wen, Jiacheng Wen, Yihua Hu, and Yang Du. Transient dc bias elimination of dual-active-bridge dc-dc converter with improved triple-phase-shift control. *IEEE Transactions on Industrial Electronics*, 67(10):8587–8598, 2020.